J. Xu[a*], SV. Lomov[a], I. Verpoest[a], S. Daggumati[b], W. Van Paepegem[b], J. Degrieck[b], M. Olave[c]

[a]Katholieke Universiteit Leuven, Department of Metallurgy and Materials Engineering, Kasteelpark Arenberg 44

B-3001 Leuven, Belgium

[b]Ghent University, Dept. of Materials Science and Engineering, Sint-Pietersnieuwstraat 41, 9000 Gent, Belgium

[c] IKERLAN Energía, Technology Park of Alava, Juan de la Cierva 1, 01510 Miñano Menor, Alava

Email: Jian.Xu@mtm.kuleuven.be

FE-Modeling of Damage of Twill Carbon/Epoxy Composite on Meso-Scale, Materials Characterization and Experimental Verification

ABSTRACT

Aim of this work is to evaluate the damage in twill carbon/epoxy composites on meso-scale level (fabric unit cell level). Averaged stiffness, Poisson ratios of pre- and post damage phase are calculated based on numerical homogenization technique with periodic boundary conditions (PBCs). The static strengths and initiation of the damage are calculated and validated by experiments. The anisotropic stiffness degradation model is implemented into Abaqus® UMAT. The algorithm of quasi-static damage is further used to model the cycles of the fatigue loading, together with the experimental S-N curves of unidirectional composite (UD), utilized as input data for the impregnated yarns. The output of the model is S-N curve of textile composites.

Keywords: meso-scale; woven composite; fatigue damage; finite elements; stiffness degradation method; multi-axial fatigue

1. INTRODUCTION

Textile reinforced composites are increasingly used many industrial fields. Fatigue design criteria of those materials are usually determined by experiments. However, due to the complex and variable architectures and design parameters of the reinforcement and considerable time consumption of the tests, a reliable numerical method for evaluation of the fatigue characterizations, fatigue endurances for instance, would be of great value.

Methodology of this work is: (a) on meso-scale FE-model, the material of the impregnated yarns represented by UD composite with known fibre volume fraction [1]; (b) anisotropic stiffness degradation method [2] is employed as stiffness degradation model both for static and fatigue damage evolution; (c) fibre fatigue and intra-fibre fatigue are separated, and the concept of multi-axial fatigue is applied to intra-fibre fatigue; (d) during the stretching of the unit cell to the maximum fatigue load, static damage algorithm is employed to simulate a whole load cycle. Some of the aspects have been mentioned in [3-4].

For the numerical static test, experimental data sets are available for validation. The data sets are collected from tests of twill carbon/epoxy composites, T3K (3K tow), which are made of HexPly® M10 prepregs.

2. FATIGUE MODELING

2.1 The Overall Algorithm

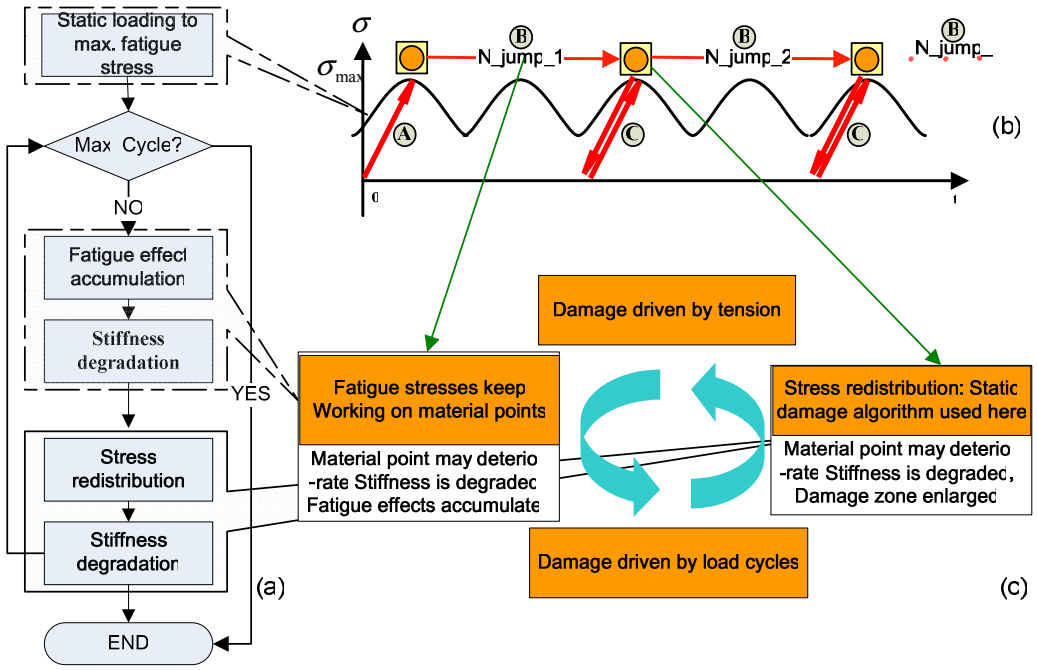

Figure 1 Sketch map of the algorithm of fatigue analysis of textile composites

The proposed approach comprises of three main computational modules: A, B and C shown in figure 1(b): (A) quasi-static loading is applied to the intact unit cell as first half cycle. During the loading increasing to σ_{max}, some material points are identified as damaged and their stiffness is degraded following exhaustively the approach presented by Zako [2] and Lomov[1]; (B) material points are being "worn out". For certain number of load cycles, *N_jump* [5] constituting as "load cycle jump", materials points have been continuously experiencing the weakening effects, which are driven by load cycle increment and the local stresses states. According to Palmgren-Miner's rule, some of the material points are identified as damaged and their stiffness is degraded; (C) static module is invoked again, simulating one load cycle. After the preceding fatigue vitiation, the unit cell will be unloaded and then reloaded to the maximum fatigue stress as one load cycle – figure 1(c). Consequence of the unloading-loading could be the enlargement of damage zones.

2.2 Fatigue Damage Initiation for UD Composite: Multi-axial Fatigue

For anisotropic material, such as textile composites, even under external uni-axial fatigue loading, locally it is multi-axially fatigued, especially after the crack onsets. Liu [6] proposed a new mode based on "critical plane" theory. The critical plane depends on the "crack plane" (plane with the maximum normal stress) and materials properties. Later, Liu [7] extended the model to anisotropic materials. To meet the requirement of 3-D stress state in yarn, the term representing out-of-plane shear ($\tau_{a,c(3)}$) [8] is added.

$$\frac{1}{\beta}\sqrt{\left[\sigma_{a,c(1)}^2\left(1+\eta_{N_f}\frac{\sigma_{m,c(1)}^2}{f_{N_f}(\theta_{\max})}\right)\right]^2+\left(\frac{f_{N_f}(\theta_{\max})}{t_{N_f}(\theta_{\max})(2)}\right)(\tau_{a,c(2)})^2+\left(\frac{f_{N_f}(\theta_{\max})}{t_{N_f}(\theta_{\max})(3)}\right)(\tau_{a,c(3)})^2+k(\sigma_{a,c}^H)^2}=f_{N_f}(\theta_{\max})$$

(1)

In Eq.1, $\sigma_{a,c(1)}$, $\sigma_{m,c(1)}$, $\sigma_{a,c}^H$, $\tau_{a,c(2)}$ and $\tau_{a,c(3)}$ stand for normal stress, mean normal stress, hydrostatic stress, in-plane shear stress and out-of-plane-shear stress amplitudes on critical plane, respectively. β, k and α are material properties related constants and angle between crack plane and critical plane, defined in TABLE I. Experimentally curve-fitted, η_{N_f} describes the effect of mean normal stress. $f_{N_f}(\theta_{\max})$, $t_{N_f}(\theta_{\max})(2)$ and $t_{N_f}(\theta_{\max})(3)$ are fatigue strengths on crack plane, which are tensile fatigue strength, in-plane shear and out-of-plane-shear strength, respectively. $\theta_{\max}$ is the angle between norm of crack plane and fibre direction. Crack plane is the micro plane which has physical crack experiencing the largest norm stress. Fatigue strengths on crack plane, which are functions of angle $\theta_{\max}$, can be calculated through Tsai-Wu strength transformation.

2.3 Quasi-static Damage Analysis

2.3.1 Mechanic Properties of the Impregnated Yarn (UD)

Yarns are locally represented as impregnated UD composite, which is considered as transversally isotropic homogeneous material. The averaged fibre volume fraction in the yarn could be obtained from the geometrical model of the reinforcement, which preserves the overall fibre volume fraction in the unit cell.

TABLE I. MATERIAL CONSTANTS FOR MULTI-AXIAL FATIGUE DAMAGE EVALUATION[6]

Material constant	$s=t(N)/f(N)\le 1$	$s>1$
α	$\cos(2\alpha)=-2+\sqrt{4-4(1/s^2-3)(5-1/s^2-4s^2)}/2(5-1/s^2-4s^2)$	$\alpha = 0$
k	$k = 0$	$k=9(s^2-1)$
β	$\beta = [\cos^2(2\alpha)s^2+\sin^2(2\alpha)]^{0.5}$	$\beta = s$

TABLE II ANISOTROPIC DAMAGE MODEL

Damage mode	Anisotropic damage model for fiber				Isotropi damage model for matrix
	Mode 1 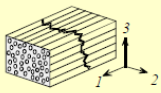	*Mode 2 & 12* 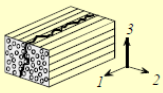	*Mode 3 & 13* 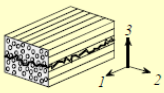	*Mode 23* 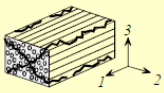	
Maximum stress-to-strength ratio	$\frac{\sigma_1^{\ 2}}{S_1^{t}\,S_1^{c}}$	$\frac{\sigma_2^{\ 2}}{S_2^{t}S_2^{c}}$ *or* $\left(\frac{\tau_{12}}{S_{12}}\right)^2$	$\frac{\sigma_3^{\ 2}}{S_3^{t}S_3^{c}}$ *or* $\left(\frac{\tau_{13}}{S_{13}}\right)^2$	$\left(\frac{\tau_{23}}{S_{23}}\right)^2$	—
Damage tensor $\begin{bmatrix} D_1 & 0 & 0 \\ 0 & D_2 & 0 \\ 0 & 0 & D_3 \end{bmatrix}$	$\begin{bmatrix} 1 & 0 & 0 \\ 0 & 0 & 0 \\ 0 & 0 & 0 \end{bmatrix}$	$\begin{bmatrix} 0 & 0 & 0 \\ 0 & 1 & 0 \\ 0 & 0 & 0 \end{bmatrix}$	$\begin{bmatrix} 0 & 0 & 0 \\ 0 & 0 & 0 \\ 0 & 0 & 1 \end{bmatrix}$	$\begin{bmatrix} 0 & 0 & 0 \\ 0 & 1 & 0 \\ 0 & 0 & 1 \end{bmatrix}$	$\begin{bmatrix} 1 & 0 & 0 \\ 0 & 1 & 0 \\ 0 & 0 & 1 \end{bmatrix}$

Yarn stiffness matrix components and Poisson ratios are calculated through Chamis' equations. Another set of properties concern the static damage initiation, the strengths. Since the strengths depend on local Vf which varies from 30% to 90%, not completely covered by existing database, the 'educated guesses' may be adopted [9-11]

2.3.2 Damage Propagation Law

The fatigue damage is captured by the multi-axial damage criterion before fibre breakage; after fibre rupture, the material point is considered to be catastrophically broken. The post-damage behavior of a material point under both static and fatigue loading is governed by the anisotropic damage mode, as shown in TABLE II. In the table, the numbers *1*, *2* and *3* are correspondent to longitudinal and two transversal directions of the material coordinate system in the fibre bundles; *t* and *c* stand for tension and compression. Mode *1* delineates fibre breakage while others are for inter-fibre cracks. The damage modes are identified by the maximum value of the stress-to-strength ratios [1-2] (see the second row of TABLE II).

TABLE III CHARACTERIZATION OF T3K

	Fibre in yarn	Yarn width (mm)	Yarn Thickness (mm)	Ends/picks (1/cm)		Total Vf	E11 (GPa)	Tensile Strength (MPa)
T3K	3K	2	0.085	4.8	Exp. Data	48.5%	65.75	867±30
					FE		60.78	849.4
					Mori-Tanaka		59.83	NA

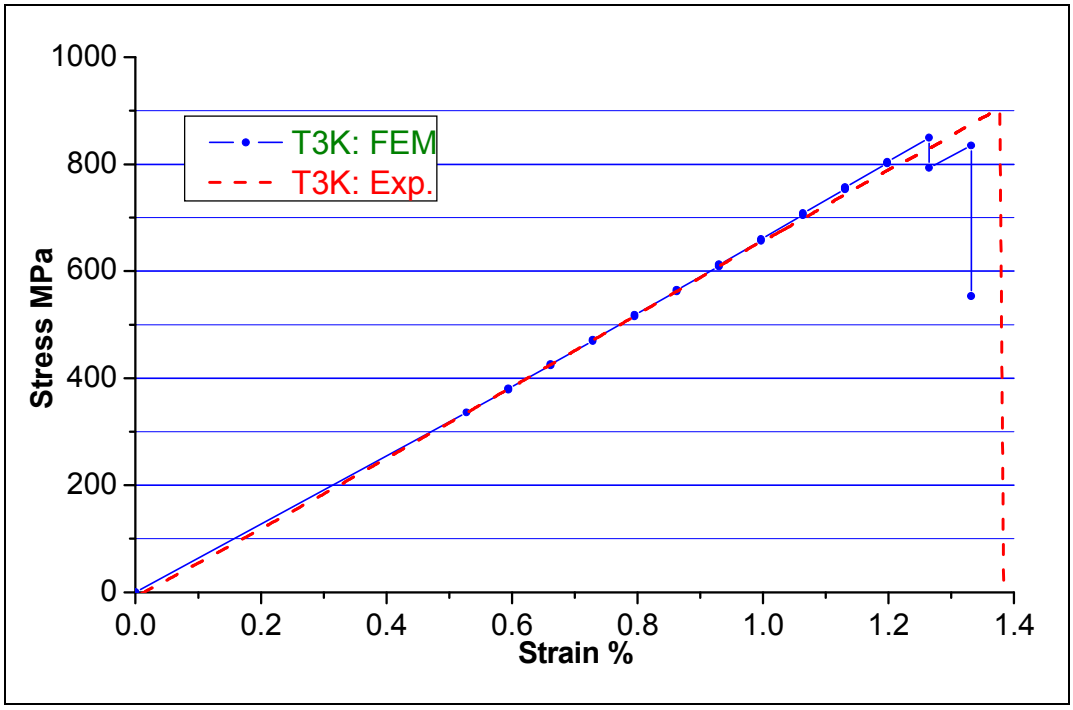

Figure 2 Computed quasi-static strain-stress diagram for PW12K-CFRP

2.3.3 Validation of the Static Damage Algorithm

The comparison of the computed results and experimental data of T3K is listed in TABLE III. The geometry is produced by the WiseTex software [12] with the parameters of the reinforcement as shown in TABLE III. Figure.2 illustrates the computed strain-stress diagram compared with test results. The Yang's modulus and strength fall into an acceptable rang –TABLE III.

3. VALIDATION OF THE FATIGUE MODEL

3.1 Materials and Input Data for Modeling

Before collecting the fatigue data from UD composite, having the same resin system with T3K, the complete test results may be obtained from literature for qualitive study. Original from [13], four sets of up-scaled T-T fatigue test data of UD composite (AS4/3501-6), delineating loading in fibre, transverse fibre, in-plane-shear and out-of-plane-shear direction, are extracted for this modeling work. Linear least square method is applied to the fatigue data curve fitting (figure 3 (b)(c)(d)) except for the data scatter in the fibre direction, for which the so-called Semi-Logarithmic-Bilinear model [14] (SLB, Eq.2) is opted as regression representation of the S-N curve:

$$\begin{cases} S = S_{static} & N \le N_1 \\ S = -A\log_{10} N + B & N_1 < N \le N_L \\ S = E & N > N_L \end{cases} \quad (2)$$

In equation 2, S and N stand for the fatigue strength and cyclic loading number respectively. A, B are constant coefficients evaluated by regression method, E is the fatigue limit. N_1 is the cycle number where the strength starts decreasing, and N_L is the cycle number correlated to the fatigue limit.

In figure 3(a), the SLB curve depicts that the fatigue strength starts drastically decreasing after ten thousand cycles and reaches the fatigue limit at about one million cycles. The coefficients *A, B* and *E* are determined by the following assumptions: the statistical distribution of the stress limits for any number of cycles follows normal distribution with the same standard deviation; they can be projected to one certain life cycle paralleling to the S-N curve. Following the idea [14], the limit N_L is iteratively being sought, and for each limit to be determined, $N_L^{'}$, all the data points are projected on the line, $N = N_L^{'}$. The curve is drawn at 50% of normal probability, and by means of normal probability paper, the correlation coefficient is computed. The $N_L^{'}$, with the maximum value of correlation coefficient (closest to 1.0), is defined as the fatigue limit, thus the associated S-N curve is attained.

3.2 Validation

Fatigue data was collected by Nishikawa [15]. Agreement between experiments and simulation are shown in figure 4. At medium stress levels, 700MPa and 650MPa, the predictions are good, and at 600MPa loading level, the data point was ‘ran-out’, which is also confirmed by the model. Slight discrepancy occurs at low-cycle fatigue. However, for high-loading fatigue, conservative prediction shows its advantages in the application.

4. CONCLUSIONS

A promising numerical method for textile composites fatigue analysis is proposed based on meso-scale level with FE method. For static analysis, averaged properties are verified through types of materials and shows good agreements. With the input data and validation data extracted from literatures, fatigue analysis shows reasonably acceptable agreements.

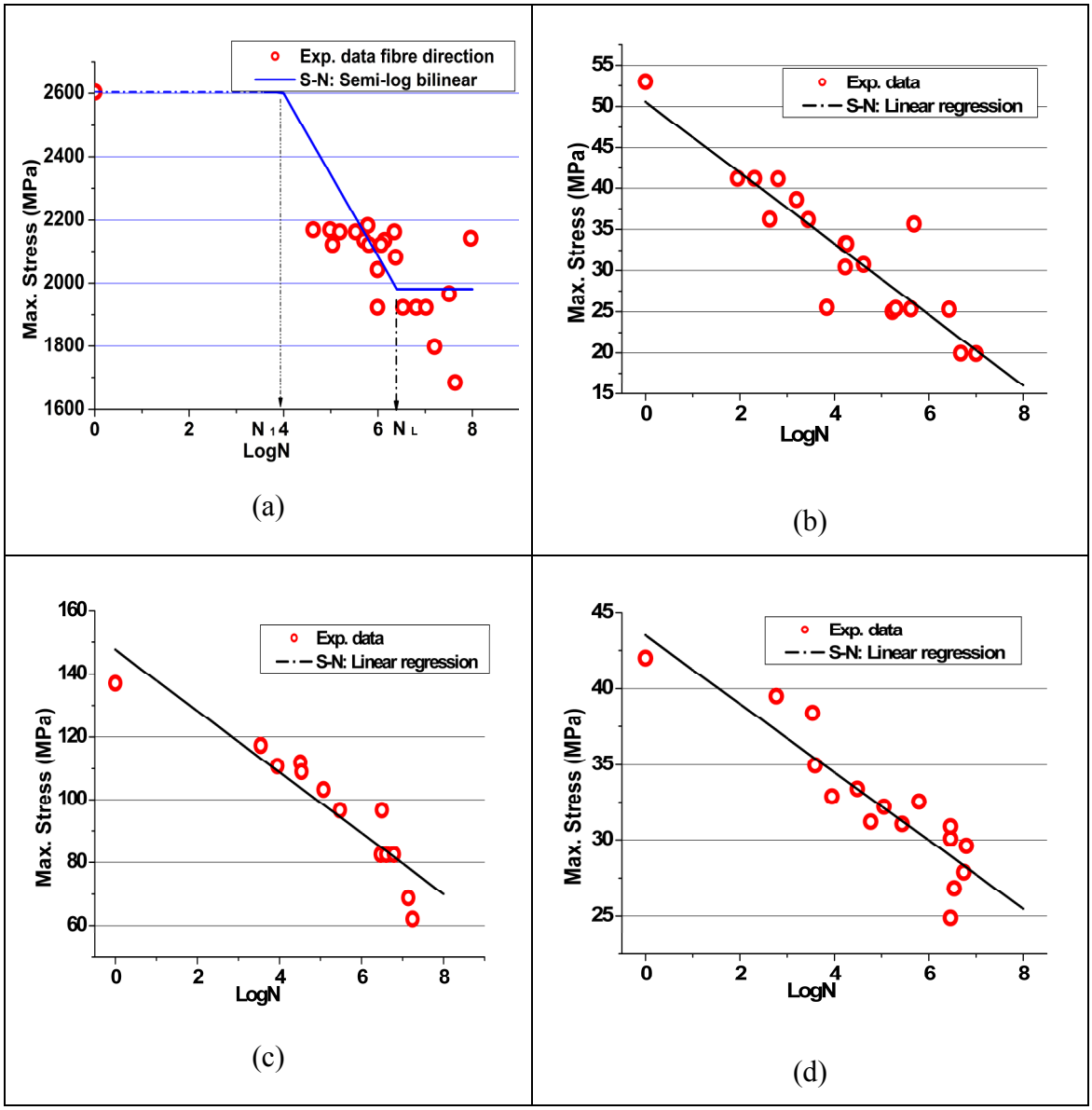

Figure 3 S-N curves of UD composite [13]: (a) fibre T-T, up-scaled from fibre volume fraction 62% to 74.4% ; (b) transverse fibre T-T; (c) in-plane shear; (d) out-of-plane shear

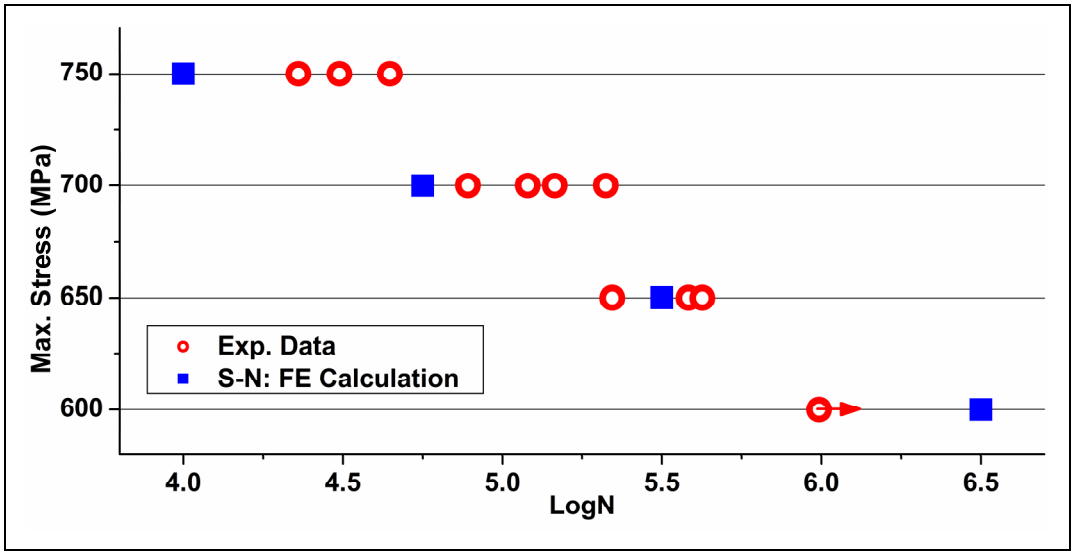

Figure 4 Validation for endurance strength

Reference List

[1] S. V. Lomov, D. S. Ivanov, I. Verpoest, M. Zako, T. Kurashiki, H. Nakai, S. Hirosawa. Meso-FE modelling of textile composites: Road map, data flow and algorithms. Composites Science and Technology. 2007;67(9):1870-1891.

[2] M. Zako, Y. Uetsuji, T. Kurashiki. Finite element analysis of damaged woven fabric composite materials. Composites Science and Technology. 2002;63(3-4):507-516.

[3] S.Hanaki, S.V.Lomov, I.Verpoest, M.Zako, H.Uchida. Estimation of fatigue life for textile composites based on fatigue test for unidirectional materials. Finite element modelling of textiles and textile composites.

[4] S.Kari, J.Crookston, A.Jones, N.Warrior, A.Long. Micro and meso scale modelling of mechanical behaviour of 3d woven composites. Proceedings of SEICO 08 SAMPE Europe International Conference.

[5] W. Van Paepegem, J. Degrieck. Fatigue degradation modelling of plain woven glass/epoxy composites. Composites Part A: Applied Science and Manufacturing. 2001;32(10):1433-1441.

[6] Y. Liu, S. Mahadevan. Multiaxial high-cycle fatigue criterion and life prediction for metals. International Journal of Fatigue. 2005;27(7):790-800.

[7] Y. Liu, S. Mahadevan. A unified multiaxial fatigue damage model for isotropic and anisotropic materials. International Journal of Fatigue. 2007;29(2):347-359.

[8] Y. Liu, B. Stratman, S. Mahadevan. Fatigue crack initiation life prediction of railroad wheels. International Journal of Fatigue. 2006;28(7):747-756.

[9] C. C. Chamis. Mechanics of Composite-Materials - Past, Present, and Future. Journal of Composites Technology & Research. 1989;11(1):3-14.

[10] B. W. Rosen. Mechanics of composite strengthening. In: Fiber Composite Materials. Metals Park (OH): ACM. 1965.

[11] T. Hirai, H. Yoshida. The effect of moulding on the mechanical properties of FRP. Journal of the Society of Materials Science, Japan|Journal of the Society of Materials Science, Japan. 1974;23(254):954-959.

[12] I. Verpoest, S. V. Lomov. Virtual textile composites software WiseTex: Integration with micro-mechanical, permeability and structural analysis. Composites Science and Technology. 2005;65(15-16):2563-2574.

[13] M. M. Shokrieh, L. B. Lessard. Progressive Fatigue Damage Modeling of Composite Materials, Part II: Material Characterization and Model Verification. Journal of Composite Materials. 2000;34(13):1081-1116.

[14] S. Hanaki, M. Yamashita, H. Uchida, M. Zako. On stochastic evaluation of S-N data based on fatigue strength distribution. International Journal of Fatigue.In Press, Corrected Proof.

[15] Y. Nishikawa, K. Okubo, T. Fujii, K. Kawabe. Fatigue crack constraint in plain-woven CFRP using newly-developed spread tows. International Journal of Fatigue. 2006;28(10):1248-1253.